

# The *Wnt-1* (*int-1*) Proto-Oncogene Is Required for Development of a Large Region of the Mouse Brain

Andrew P. McMahon\* and Allan Bradley†

\* Department of Cell and Developmental Biology  
Roche Institute of Molecular Biology  
Roche Research Center  
Nutley, New Jersey 07110  
† Institute for Molecular Genetics  
Baylor College of Medicine  
Houston, Texas 77030

## Summary

The *Wnt-1* (*int-1*) proto-oncogene, which encodes a putative signaling molecule, is expressed exclusively in the developing central nervous system and adult testes. To examine the role of *Wnt-1*, we generated six independent embryonic stem cell lines in which insertion of a *neo<sup>R</sup>* gene by homologous recombination inactivated a *Wnt-1* allele. Germline chimeras were generated from two lines, and progeny from matings between heterozygous parents were examined. In all day 9.5 fetuses homozygous for mutated *Wnt-1* alleles, most of the midbrain and some rostral metencephalon were absent. The remainder of the neural tube and all other tissues were normal. In late-gestation homozygotes, there was virtually no midbrain and no cerebellum, while the rest of the fetus was normal. Homozygotes are born, but die within 24 hr. Thus the normal role of *Wnt-1* is in determination or subsequent development of a specific region of the central nervous system.

## Introduction

The central nervous system (CNS) of all vertebrates has a distinct rostrocaudal and dorsoventral organization. However, the patterning processes responsible for this arrangement are, at best, poorly defined. A number of genes, whose Drosophila homologs regulate segmental pattern, are expressed in the mammalian neural tube in spatially and temporally restricted patterns, consistent with a role in the early organization of this structure. One such gene is the proto-oncogene *Wnt-1* (*int-1*).

*Wnt-1* was originally identified in several mouse mammary tumors induced by mouse mammary tumor virus (MMTV; Nusse and Varmus, 1982). Proviral integration activates the normally silent gene, leading to expression of RNA encoding an unmodified *Wnt-1* protein (van Ooyen and Nusse, 1984; for review see Nusse, 1988). Direct evidence for a transforming role has come from transgenic mouse studies that essentially recapitulate naturally occurring MMTV integration (Tsukamoto et al., 1988). Thus, deregulated *Wnt-1* expression can have profound consequences on the organization and growth of responsive tissues.

Normal expression of *Wnt-1* in the mouse is limited to haploid round spermatids in adult testis (Jakobovits et al.,

1986; Shackleford and Varmus, 1987) and to the developing CNS in the fetus (Shackleford and Varmus, 1987; Wilkinson et al., 1987a). In situ hybridization failed to detect *Wnt-1* expression prior to induction of the neural plate (Wilkinson et al., 1987a). However, shortly thereafter, RNA transcripts are found exclusively in the open neural plate of the early somite-stage embryo at 8.5 days (Wilkinson et al., 1987a). At this time, the rostral limit lies in the region of the presumptive midbrain, the caudal limit in the presumptive hindbrain. Rostrally, transcripts are expressed throughout the neural plate; caudally, they are restricted to the lateral margins of the neural plate, which forms the dorsal midline on closure of the neural tube. By 9.5 days (20–27 somites) expression extends from the midbrain caudally along the length of the neural tube and is localized at the dorsal midline of the midbrain, the spinal cord, and the equivalent cells of the myelencephalon that are displaced laterally by the ependymal roof. The two major exceptions to the continuous dorsal midline expression are a region of caudal metencephalon, which does not express *Wnt-1*, and a circle of expressing cells at the midbrain–hindbrain junction. The pattern established at 9.5 days remains essentially unmodified, except for distortions due to morphogenetic movements, until at least 14.5 days (Wilkinson et al., 1987a, 1989). As the *Wnt-1* protein is secreted, at least in cell culture (Papkoff, 1989; Papkoff and Schryver, 1990; Bradley and Brown, 1990), *Wnt-1* presumably regulates some aspect of cell–cell interactions in early neural development. Studies on the Drosophila counterpart of *Wnt-1* suggest that this role is likely to be quite significant.

The Drosophila *Wnt-1* protein is encoded by the segment polarity gene (Nüsslein-Volhard and Wieschaus, 1980) *wingless* (*wg*; Sharma, 1973; Sharma and Chopra, 1976; Baker, 1987; Cabrera et al., 1987; Rijsewijk et al., 1987). Like other members of this class of genes, *wg* is essential for normal patterning in each segment (Nüsslein-Volhard and Wieschaus, 1980; Baker, 1987, 1988). Loss of *wg* expression results in the loss of naked cuticle, a posterior segmental pattern element, and replacement by mirror-image duplication of anterior denticles bands. The non-cell-autonomous action of *wg* mutations (Morata and Lawrence, 1977; Baker, 1988) initially suggested that *wg* may be secreted, a view that has been substantiated by direct immunological localization (van den Heuvel et al., 1989). The secreted *wg* protein acts on neighboring cells, at least in part, to regulate expression of another segmentation gene, the homeobox-containing gene *engrailed* (DiNardo et al., 1988; Martinez-Arias et al., 1988). Given that Drosophila *Wnt-1* regulates pattern, and expression of the mammalian gene is both temporally and spatially consistent with a patterning role in neural development, we have suggested that *Wnt-1* in the mouse may regulate pattern in the developing CNS (McMahon and Moon, 1989).

To test this hypothesis, we have generated null alleles of *Wnt-1* by homologous recombination (Thomas and Capecchi, 1987) in embryonic stem (ES) cells (Evans and

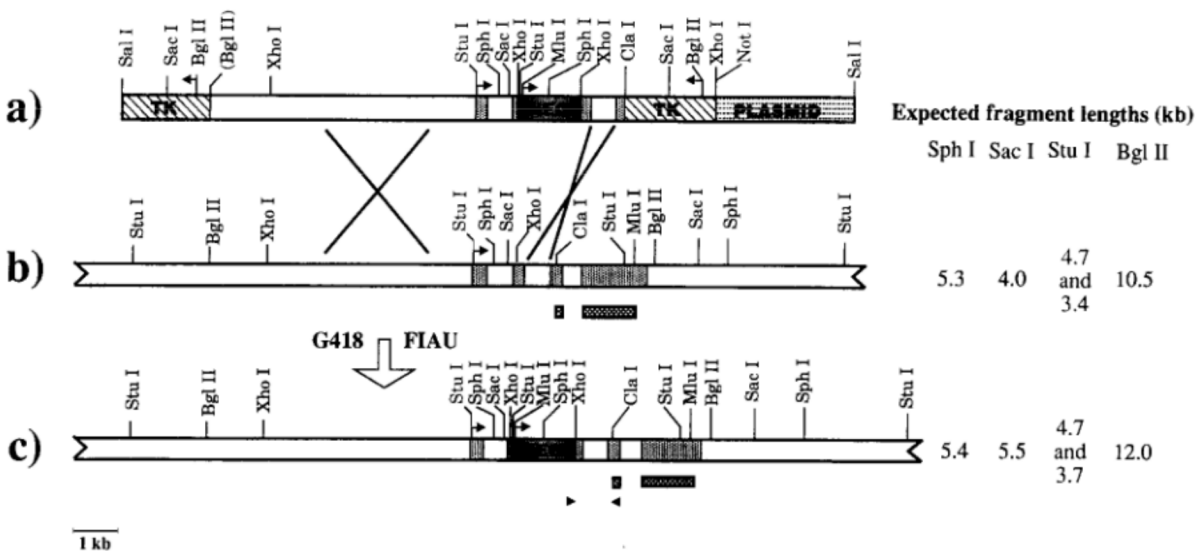


**Figure 1.** Schematic Representation of the *Wnt-1* Targeting Vector and Recombination at the *Wnt-1* Locus

(a) Restriction map of the *Wnt-1* homologous recombination construct, p401. The plasmid contains approximately 7.5 kb of homology 5' and 921 bp 3' of the *neo* insertion, which interrupts the *Wnt-1* coding sequence within the second exon. *Wnt-1* genomic sequences are flanked on either end by MC1-tk sequences. Arrows indicate transcriptional orientation of the *Wnt-1*, tk, and *neo* promoters.

(b) Restriction map of the wild-type *Wnt-1* locus in the region homologous to p401. Hatched boxes indicate exonic regions homologous to the diagnostic *Wnt-1* cDNA probe (Clal-MluI) used to identify *Wnt-1* alleles in Southern blots.

(c) The predicted structure of a mutated *Wnt-1* allele following homologous recombination with p401. Hatched boxes represent exonic regions homologous to the diagnostic *Wnt-1* cDNA probe. Filled arrowheads indicate approximate positions of oligonucleotide sequences used to identify allele-specific recombination. The left oligonucleotide sequence lies within the rat  $\beta$ -actin sequences at the 3' end of the *neo* cassette. The right oligonucleotide sequence lies within coding sequence in the third exon, just 3' of the *Cla*I site that marks the 3' boundary of *Wnt-1* sequences in p401. The expected sizes of restriction fragments detected by the *Wnt-1* diagnostic cDNA probe on Southern analysis of digests of normal (b) and targeted (c) *Wnt-1* alleles are indicated.

Kaufman, 1981) and have used these to generate mouse lines (Bradley et al., 1984). Examination of homozygous *Wnt-1* mutant fetuses indicates that *Wnt-1* is required for normal development of a large domain of the CNS encompassing much of the midbrain and rostral metencephalon. These findings support the view that *Wnt-1* plays a major role in either the establishment or subsequent development of brain-forming regions of the neural plate.

## Results

## **Homologous Recombination at the *Wnt-1* Locus**

The feasibility of generating and detecting gene targeting events at the *Wnt-1* locus in ES cells depends on both the innate targeting frequency and expression of a *neo* resistance gene integrated at that locus. Transcription from the widely used *neo* cassette for gene targeting in ES cells, pMC1neopA (Thomas and Capecchi, 1987), is very position dependent. Since *Wnt-1* is not expressed at detectable levels in ES cells, there was the possibility that pMC1neopA would not express at an adequate level, in a "silent" locus, to generate a G418<sup>R</sup> cell following homologous integration.

We have tested pMC1neopA by transfection in the context of a number of different vectors and identified one vector that fortuitously gave an 11-fold enhanced transfection efficiency relative to pMC1neopA alone. This vector contains approximately 300 bp of rat  $\beta$ -actin promoter se-

quence 3' of *neo*, which presumably acts to enhance *neo* transcription, reducing the influence of the integration site on *neo* expression. The Xhol MC1neopA- $\beta$ -actin fragment was inserted into a Xhol site within codons 57 and 58 in the second exon of a *Wnt-1* genomic subclone (Figure 1). As this effectively separates the signal peptide at the amino terminus from the most conserved amino acids found after position 100 in the predicted protein sequence, homologous recombination of this clone at the *Wnt-1* locus would almost certainly generate a null allele. The *Wnt-1* homologous recombination construct, p401, contains 921 bp of homology 3' and approximately 7.5 kb 5' of the *neo* insertion (Figure 1). To select against random integration events, we incorporated two herpes simplex virus thymidine kinase (HSV-tk) genes, one on either end of the targeting vector (Mansour et al., 1988). These were driven by the same promoter and polyoma enhancer that drive the *neo* cassette, although they do not have the 3' actin enhancer elements (Figure 1).

p401 was transfected into  $2.2 \times 10^8$  AB-1 ES cells, and the transfected population was plated onto SNL76/7 feeder cells. Simultaneous selection in G418 and the pyrimidine derivative FIAU was initiated 24 hr after plating. G418<sup>R</sup> and FIAU<sup>R</sup> colonies were detected after 9–10 days, with an average of 75 per plate. FIAU selection produced a 26-fold enrichment for targeted integration events over random integration events. To detect homologous recombinant clones, we used PCR primers specific for a

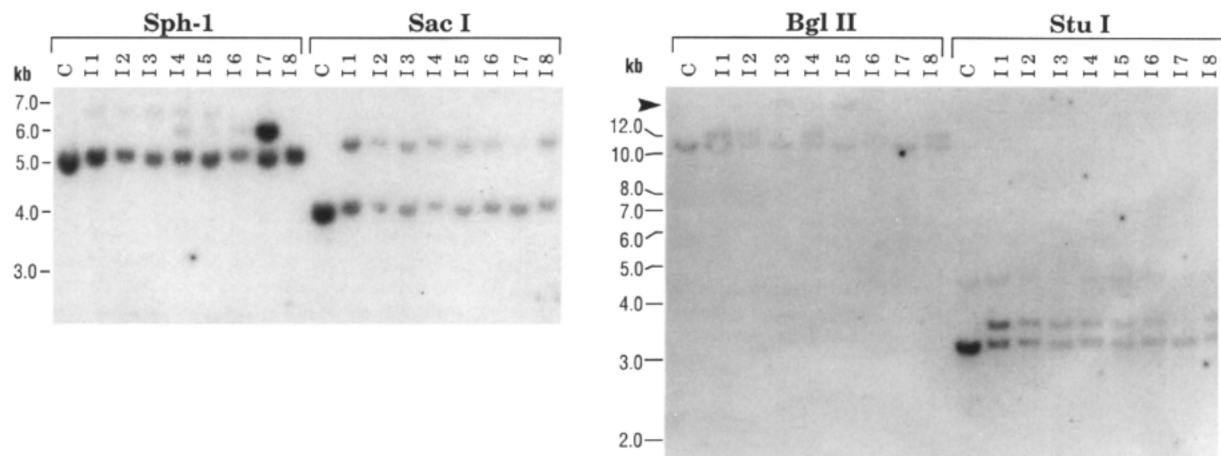


Figure 2. Southern Blot Analysis of Restriction Digests of DNA from Targeted *Wnt* ES Cell Clones

DNA samples from control (AB-1 cells untransfected) and eight targeted cell lines (I1–I8) were digested with the indicated restriction enzymes and probed with the 3' diagnostic *Wnt-1* cDNA probe. Arrowheads indicate the large BglII bands in the I3 and I5 digests that result from 5' rearrangement at the targeted locus.

junction fragment present at the 3' end of the construct (Figure 1). PCR primers were generated for actin sequences at the end of the *neo* cassette and for *Wnt-1* genomic sequences that lie just 3' of the *Cla*I site, which marks the end of homology. Tests indicated that the correct 1025 bp 3' junction fragment was detected on ethidium bromide-stained gels following amplification of only 10 single-copy equivalents in the presence of genomic DNA from  $10^4$  wild-type cells (data not shown).

Colonies were screened by the half-colony method (Joyner et al., 1989) in pools of 30–90. Each pool represented colonies from either a half or a complete plate. From 39 pools screened (representing approximately 1650 clones), six positive pools were identified on ethidium bromide-stained agarose gels and confirmed by hybridization to an internal probe (data not shown). Four of the pools yielded single positive clones. The two remaining pools yielded two positive clones each. Since these secondary positive clones were derived from the same plates, and the colonies on these plates had been disturbed during the initial screen, these clones cannot be unambiguously identified as independent targeting events. The frequency of gene targeting (assuming six positives) in this case was 1/275 G418<sup>R</sup> + FIAU<sup>R</sup> clones, which equates to 1/7167 G418<sup>R</sup> clones. Since there are often considerable differences in *neo*<sup>R</sup> background transfection efficiencies associated with position-dependent G418<sup>R</sup> neomycin resistance genes, the targeting frequency is best expressed per cell transfected. For *Wnt-1* this is  $1/3.6 \times 10^7$  cells transfected.

DNA from the eight lines was examined by Southern blot analysis to confirm homologous recombination and to examine in some detail the recombination event. DNA was digested with Sph I, Sac I, Stu I, and Bgl II and probed with a flanking *Wnt-1* cDNA probe that hybridizes to *Wnt-1* genomic sequences 3' of the *Cla*I site in p401 (Figures 1 and 2). Analysis of the resultant Southern blots detected

homologous recombination events in all clones (Figures 1 and 2). Sac I and Stu I produce distinct restriction fragments that distinguish the targeted from the wild-type *Wnt-1* allele. All clones showed the predicted restriction fragments generated by the normal allele. In addition, all clones have the expected fragments predicted following homologous recombination. Moreover, as would be expected, hybridization to fragments from both wild-type and recombinant alleles is of approximately equal intensity and half that of the single fragment from untransfected cells (Figures 1 and 2). The wild-type and targeted alleles have similar-sized Sph I fragments that are not resolved under these conditions. The signal intensity relative to other digests clearly indicates that both Sph I fragments are comigrating, an observation confirmed by hybridization with a *neo* probe to detect the Sph I fragment from the targeted allele (data not shown). Thus recombination at the 3' end of the region of homology is apparently normal. Consistently, one clone, I7, showed lower levels of hybridization to the mutant allele, although the reason for this is unclear.

As Bgl II cuts at the end of the 5' region of homology, this provides a useful means to examine the fidelity of recombination 5' of the *neo* sequences. All clones, other than I3 and I5, had the predicted fragments generated by the normal (10.5 kb) and targeted (12.0 kb) alleles (Figures 1 and 2). In contrast, I3 and I5 have a larger Bgl II fragment than expected, presumably as a result of a 5' rearrangement (Figures 1 and 2). Thus, at this level of resolution, six of the eight lines show faithful homologous recombination with no detectable rearrangements.

To examine these clones further, DNA digests were probed with *neo* and tk probes. As expected, tk sequences, which should be deleted on recombination, were not detected in any sample (data not shown). Moreover, hybridization with a *neo* probe failed to detect any bands in addition to those predicted (data not shown).

Table 1. Generation of Chimeric Males and Germline Transmission of Targeted *Wnt-1* Alleles

Clone	Embryos Injected	Born	Chimeric Males	Chimeric Females	Average Extent ES-Derived Contribution	Males Scored for Germline Transmission	Germline Chimeras	Complete Transmitters
2	34	12	12	0	95%	10	10	4
3	26	11	10	1	95%	10	9	6
7	15	4	2	1	80%	ND		

Survival to term was 45%, which is within the range observed for AB1 clonal isolates in combination with C57 blastocysts. All of the animals scored were chimeric. Five additional offspring were born but did not survive to day 10, when the ES cell-derived agouti color is detectable in the hair. Ten of the I2 chimeras and all of the I3 chimeras were bred. All males proved fertile. All germ cells are ES cell derived in complete transmitters as a result of sex conversion. A high contribution of XY ES cells in an XX host results in testis formation. As XX germ cells do not form viable sperm, all sperm are ES cell derived, hence the complete transmission of the ES cell genome. ND, not done.

Thus, all clones are the result of a single integration event that occurred at the *Wnt-1* locus.

#### Heterozygous *Wnt-1* Cell Lines Efficiently Make Germline Chimeras

The culture and clonal isolation of ES cells with the desired homologous genetic exchange might result in selection for random undesired genetic changes that have arisen spontaneously in culture. To avoid such potential artifacts, we elected to generate germline transmission and study homozygous animals from a minimum of two independent clones. Heterozygous clones representing three independent targeting events were injected into C57BL/6 (C57) host blastocysts. The results are presented in Table 1.

All animals scored were highly chimeric. The average ES contribution, estimated by the amount of agouti pigmentation in the coat, averaged 95% for the entire experimental series. As expected, the high contribution of XY ES cells in combination with random XX and XY host embryos (Bradley et al., 1984) has resulted in a large sex bias in the resulting litters; 93% of the animals scored at term were male. Two of the clones (I2 and I3) generated a large number of chimeric males, so chimeras from these were chosen for further analysis. Chimeras from clone I7, although equally extensive, were not studied further. The male chimeras made from clones I3 and I2 were mated with C57 females. All of the males were fertile. From 20 males screened, 19 have shown germline transmission (Table 1). Heterozygosity at the *Wnt-1* locus has no discernible effect on breeding performance of the chimeric males, despite the expression of *Wnt-1* in the testes (Shackleford and Varmus, 1987).

#### *Wnt-1* Homozygous Mutants Lack a Large Region of the Brain

Intercrosses were set up between mice heterozygous for mutated *Wnt-1* alleles. As *Wnt-1* is first expressed during early stages of neural development, progeny were initially examined at 9.5 days of development, shortly after neural tube closure. At this time, the primitive brain consists of five major regions. The forebrain is composed of the rapidly expanding telencephalon, which gives rise to the cerebral cortex and basal ganglia, as well as the diencephalon, which later forms (among other structures) the

thalamus. The diencephalon connects directly to the midbrain, or mesencephalon, which in turn connects to the hindbrain. The hindbrain comprises a short metencephalon and a more extensive segmented myelencephalon caudally. The metencephalon is responsible for forming most of the cerebellum dorsally and the pons ventrally. The myelencephalon gives rise to the medulla oblongata.

Twenty-five offspring were examined from matings between mice heterozygous for the I2-derived mutant *Wnt-1* allele. Eight of these (32%, Table 2) showed a clear, invariant phenotype (Figure 3). In these individuals most of the neural tube and all nonneuronal tissues were normal. However, a substantial portion of the midbrain had failed to develop (Figure 3). A closer examination of bisected embryos revealed that the metencephalic rhombomere I was also shorter, indicating an absence of metencephalic tissue (data not shown). Histological sections confirmed that the telencephalon, diencephalon, and myelencephalon were normal and metencephalic tissue was present (Figure 3). Thus, the simplest explanation for the observed phenotype is that a large contiguous domain, comprising approximately the caudal two-thirds of the midbrain, the normal midbrain-metencephalic junction, and rostral metencephalon, failed to develop. As there is no apparent compensatory growth by other brain regions, the absence of this tissue moves the forebrain caudally, resulting in a

Table 2. Frequency of Progeny with Midbrain-Metencephalon Deficiency in Crosses between Mice Heterozygous for Mutated *Wnt-1* Alleles

	I2		I3	
	Normal	Mutant	Normal	Mutant
E9.5	17	8 (32)	ND	ND
E14.5	ND	ND	8	1 (11)
E16.5	6	1 (14)	12	6 (23)
P1	12	3 (20)	17	4 (19)
Total:	35	12 (25)	37	11 (23)

The phenotypes of progeny resulting from intercrosses between heterozygous individuals generated from the I2 and I3 clones were scored on the indicated embryonic (E) and postpartum (P) days. Figures in parentheses represent percentages. Normal offspring consist of the +/+ and +/- individuals; abnormal offspring are -/- . The overall frequency of mutants for both lines is 23/95 (24%). ND, not done.

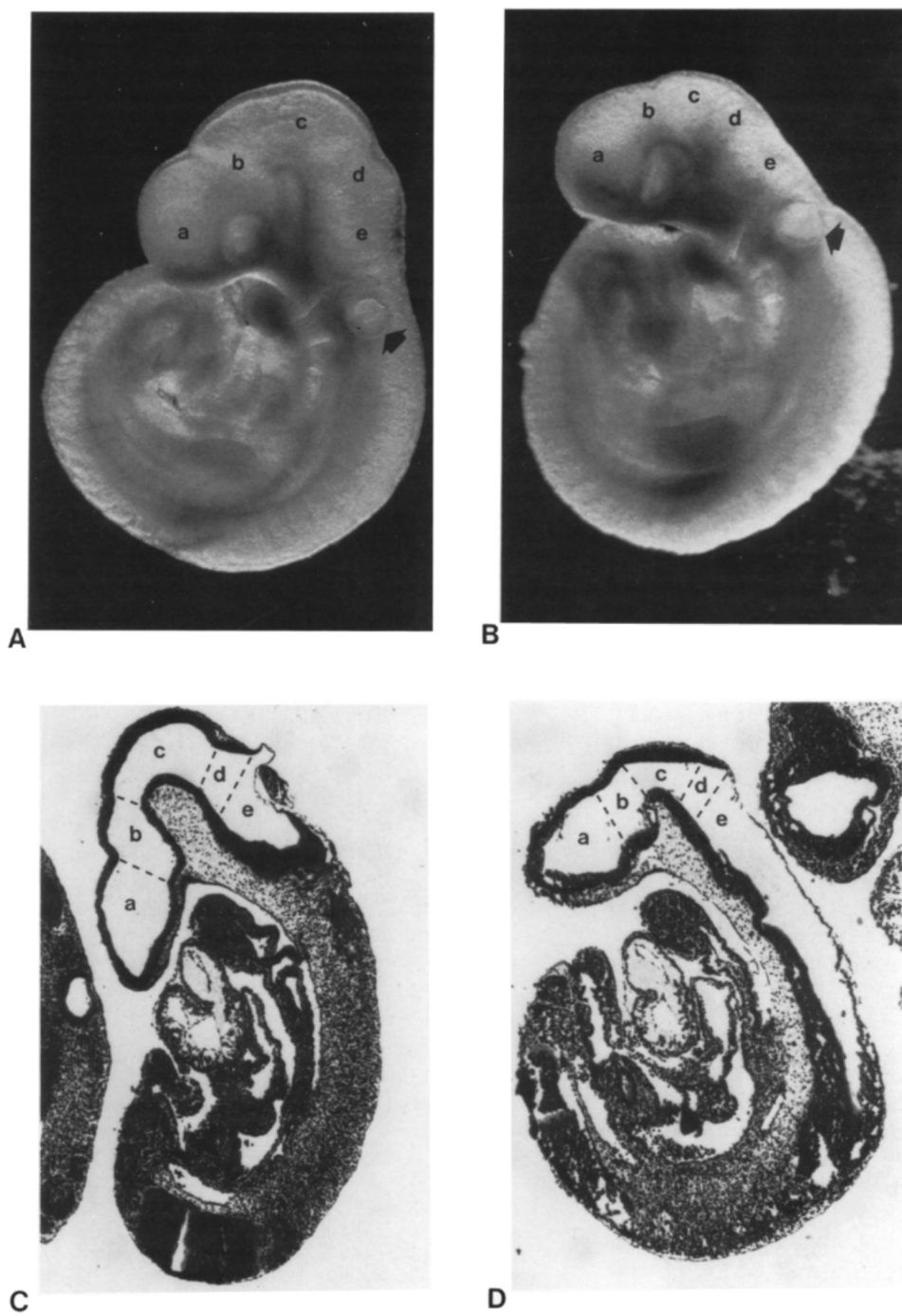


**Figure 3. Day 9.5 Littermates from Matings between Mice Heterozygous for the I2-Derived Mutated *Wnt-1* Allele**  
(A, B) Whole view of 27-somite fetuses heterozygous (A) and homozygous (B) for the mutated *Wnt-1* allele. (C, D) Parasagittal (C) and midsagittal (D) sections through fetuses heterozygous (C) and homozygous (D) for the mutated allele. The various regions of the developing brain are indicated: a, telencephalon; b, diencephalon; c, midbrain; d, metencephalon; e, myelencephalon. Arrows indicate the position of the otic vesicle, which occurs at the level of rhombomeres 5 and 6 in the myelencephalon.

new juxtaposition of rostral midbrain with caudal metencephalon.

The frequency at which this phenotype was observed (32% of progeny) is consistent with the expected frequency of homozygous individuals (25% of progeny), assuming normal Mendelian inheritance of the mutated *Wnt-1*

allele. To prove that mutants were indeed homozygous for this allele, yolk sac DNA was isolated, digested with *SacI*, and probed with the diagnostic *Wnt-1* flanking probe as described earlier. Of the five embryos examined at 9.5 days, the two homozygous for the mutated *Wnt-1* allele (I2-5 and I2-8, Figure 4) were the only progeny exhibiting the

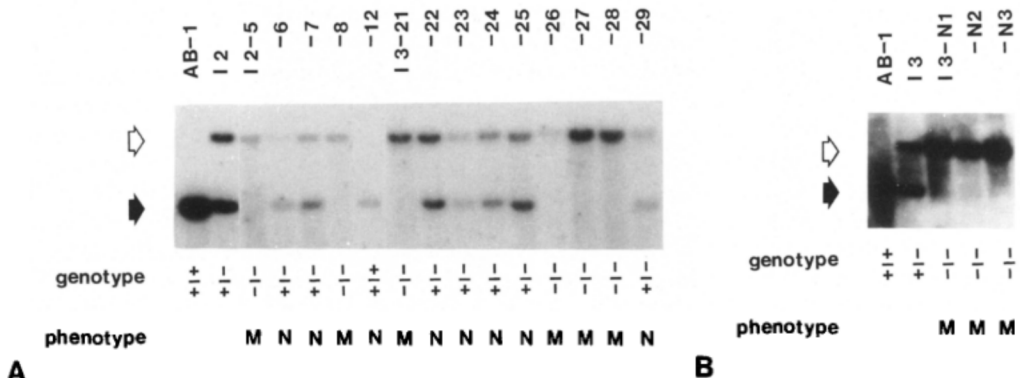


**Figure 4. Genotypic Identification of Offspring from Matings between Mice Heterozygous for I2- and I3-Derived Mutated *Wnt-1* Alleles**  
(A) Southern blot analysis of *SacI*-digested DNA isolated from the untransfected AB-1 ES cell line, from the parental I2 ES cell line, and from yolk sac DNA of offspring. I2-5 to I2-8 and I2-12: day 9.5 offspring from parental matings between I2-derived heterozygotes. I3-21 to I3-29: day 16.5 littermates from matings between I3-derived heterozygotes.  
(B) Genotypic identification of three phenotypically abnormal neonates from matings between I3-derived heterozygotes. Open arrow indicates the position of the mutated *Wnt-1* band; solid arrow indicates the position of the wild-type band. The genotypes and phenotype (M, mutant; N, normal) are indicated below.

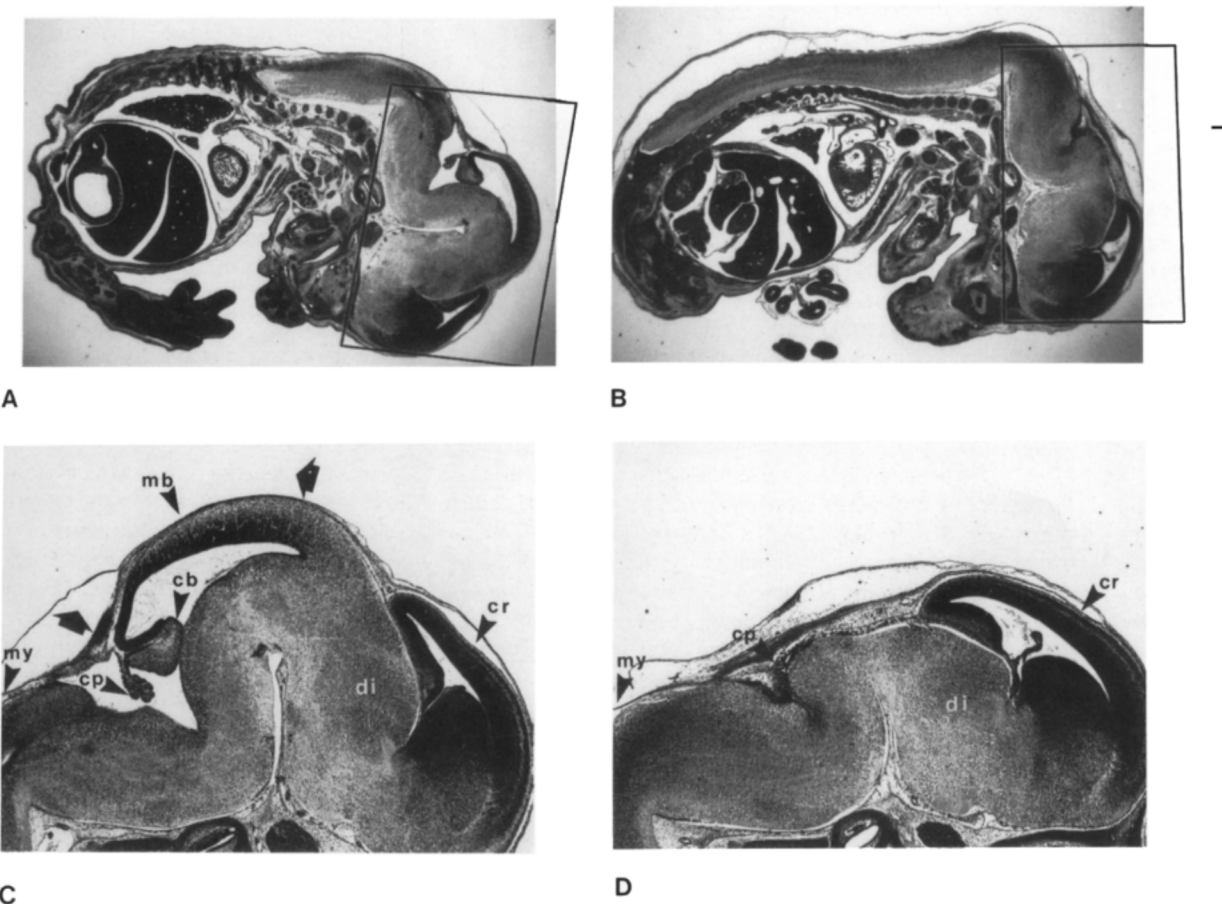


**Figure 5. Histological Section through Day 14.5 Littermates from a Mating between Mice Heterozygous for the I3-Derived Mutated *Wnt-1* Allele**  
(A, B) Sagittal views of normal (A) and mutant (B) fetuses. (C, D) Close-up views of areas boxed in (A) and (B). All tissues are normal outside of the boxed regions in (A) and (B). (C) The normal fetus has a well-developed cerebral hemisphere (cr), diencephalon (di), and midbrain (mb). In addition, by 14.5 days the cerebellum (cb) has formed from dorsal metencephalon. Behind this, the posterior choroid plexus (cp) marks the metencephalic-myelencephalic (my) junction. The approximate region deleted in the mutant littermate is indicated by the two large arrows. (D) The mutant lacks most, if not all, of the midbrain and has no obvious cerebellum. The posterior choroid plexus is present and the cerebral hemisphere, diencephalon, and myelencephalon are normal. Photographs of normal and mutant embryos were taken at the same magnification.

mutant phenotype. Thus, these early studies indicate that *Wnt-1* is required for normal development of a substantial region of the primitive brain. Analysis of later fetal stages suggests that this is its only function.

To extend this study, we investigated fetal development at 14.5 and 16.5 days. By this time, CNS development is advanced. Several convenient morphological markers distinguish brain regions and allow an unambiguous assessment of deleted areas, as well as the normality of remaining tissue. Offspring were examined from crosses between mice heterozygous for both the I2- and I3-derived mutated *Wnt-1* alleles (Table 2). Both the frequency of mutant progeny and the phenotype of mutant offspring were indistinguishable in these lines. As these alleles originated from two entirely independent homologous-recombination events, this strongly suggests that the phenotype observed is a result of mutation of only the *Wnt-1* gene.

By 14.5 days postcoitum, all major organ rudiments are laid down and many are well differentiated. We examined a single litter at this stage that contained one mutant fetus (Table 2). Histological analysis of this mutant and a normal littermate failed to detect any abnormality outside of the CNS (Figure 5). Moreover, as observed at 9.5 days, all the CNS was apparently normal with the exception of the midbrain and metencephalon. The mutant fetus had little discernible midbrain (Figure 5), which is easily identifiable by its position at the "top" of the brain in the normal fetus (Figure 5). Moreover, the cerebellum, which is derived from both the caudal midbrain and rostral metencephalon (Hallonet et al., 1990), was absent (Figure 5), confirming that the deleted region extends into the metencephalon. The posterior choroid plexus, which originates at the metencephalic-myelencephalic junction, was present (Figure 5). Thus the deleted region lies rostral to this boundary. The presence of the trigeminal nerve, which exits from the rostral myelencephalon, also supports the conclusion that rostral myelencephalic tissue was unaffected (data not shown).

No decrease in the ratio of mutant to normal fetuses was observed at 16.5 days, indicating, as expected, that a localized abnormality in the developing CNS does not compromise *in utero* development. DNA from the yolk sacs of several I3-derived offspring was examined, and complete concordance between mutant phenotype and homozygosity for the I3-derived mutated *Wnt-1* allele was observed (Figure 4). Fetuses appeared superficially normal, apart from an abnormal cranial flexure due to loss of neural tissue. Brains were dissected and examined superficially and histologically (Figure 6). Even at this late stage of gestation, no abnormalities were seen outside of the midbrain and rostral metencephalon. The thalamus, a marker for the diencephalon, was readily distinguishable and appears normal (Figure 6). Moreover, the pons, which like the major part of the cerebellum is derived from the metencephalon, was normal (Figure 6). Thus, in line with the initial observations at 9.5 days, not all the metencephalic tissue was absent, though clearly the tissue that contributes to the cerebellum was missing. As at 14.5 days, wild-type and heterozygous fetuses have a well-developed cerebellum, while fetuses homozygous for the

mutant alleles have no identifiable cerebellar tissue (Figure 6).

The deletion of such a large area of the CNS would be expected to severely compromise postpartum development. Several litters were allowed to come to term, but no mutant offspring survived longer than 24 hr. Mutants were easily recognizable by their abnormal cranial flexure; however, their genotypic identity was confirmed by Southern analysis (Figure 4) and brain dissection (data not shown). The number of abnormal pups did not deviate significantly from the expected one-quarter of the offspring. Taking all the progeny from both lines at all stages, 23 of the 95 showed the "midbrainless" phenotype, in almost perfect agreement with Mendelian predictions.

## Discussion

### Homologous Recombination and Germline Transmission

The success of gene targeting at the *Wnt-1* locus and transmission of targeted alleles through the germline was dependent on several factors. The modified *neo* cassette proved much less position dependent than MC1*neo* (Thomas and Capecchi, 1987), ensuring that *neo* was expressed at the *Wnt-1* locus, which is silent in ES cells. In addition, we utilized tk sequences for negative selection against random integration events (Mansour et al., 1988). The tk sequences were incorporated at both ends of the *Wnt-1* sequence in the targeting vector. Surprisingly, this resulted in only a slightly enhanced enrichment for targeting events compared with a similar construct containing a single tk (Bradley and McMahon, unpublished data). The enrichment factor we report is considerably lower than those reported by others (Mansour et al., 1988; Johnson et al., 1989) but in line with results seen with multiple vectors designed to target other loci (Bradley, unpublished data). This difference may be due in part to the selection scheme. We have used FIAU, which has a broad spectrum in its effective-to-cytotoxic ratio, with no discernible non-specific cytotoxicity at the effective concentrations. Others have used gangcyclovir (Mansour et al., 1988; Johnson et al., 1989), which may have a higher non-specific cytotoxicity at the effective concentrations. However, DeChiara et al. (1990) used identical gangcyclovir negative selection to obtain frequencies similar to the results reported here. While the reason for these discrepancies is unclear, one variable is probably random breakage of DNA on transfection, which results in the loss of flanking tk sequences (Zijlstra et al., 1989).

The absolute frequency of targeting at the *Wnt-1* locus was low, 1 in  $3.6 \times 10^7$  treated cells. One simple explanation for this result is that the targeting frequency may depend on the transcriptional activity of the locus in ES cells. However, comparison of published (Thomas and Capecchi, 1987; Mansour et al., 1988; Johnson et al., 1989; Joyner et al., 1989; Koller and Smithies, 1989; Thompson et al., 1989; Zijlstra et al., 1989; Charron et al., 1990; DeChiara et al., 1990) and unpublished data (Bradley, unpublished data) does not support a direct correlation. Clarification of the parameters that govern the targeting

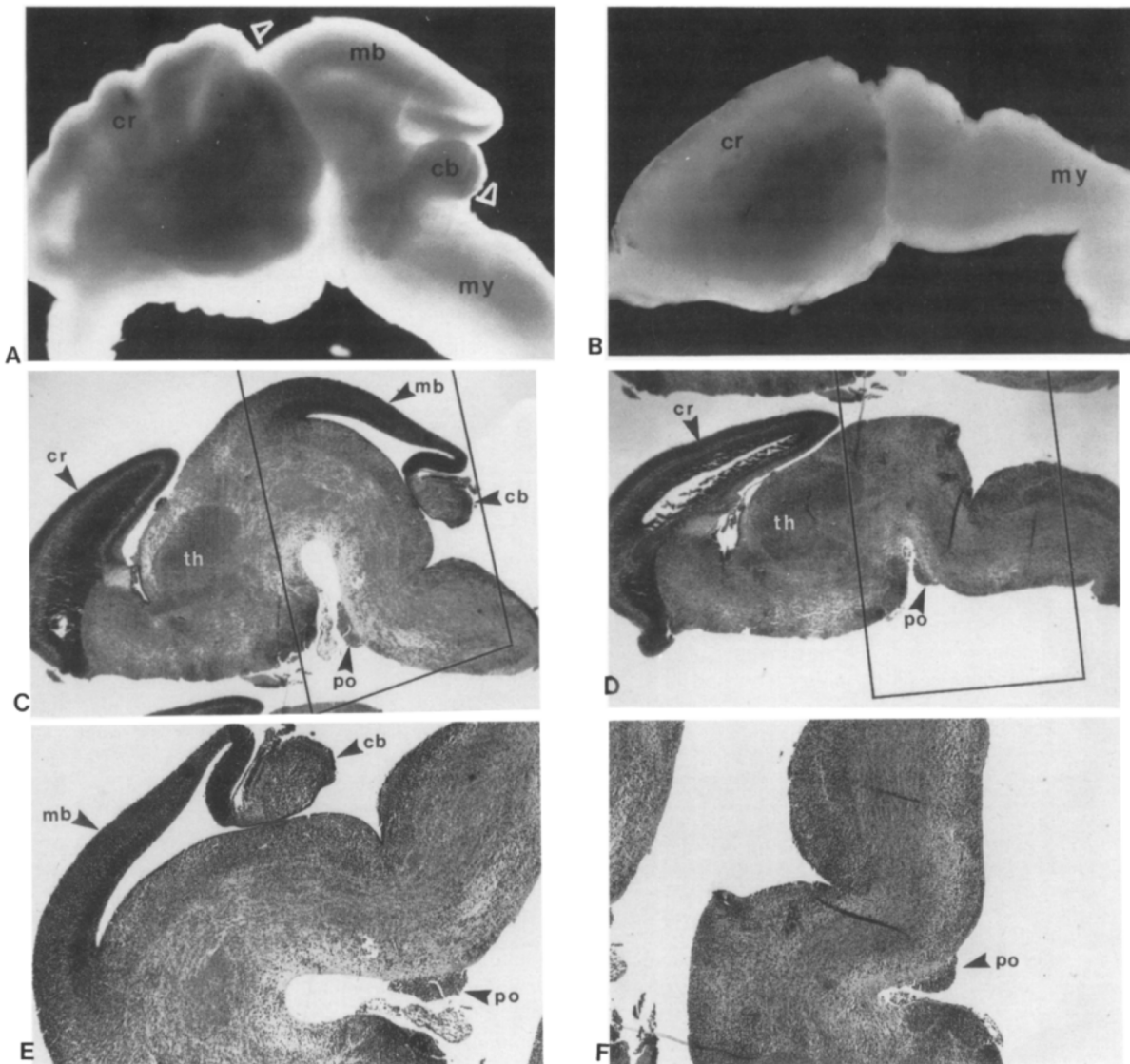


**Figure 6.** Structure of Brains in Day 16.5 Littermates from Matings between Mice Heterozygous for the I2-Derived Mutated *Wnt-1* Allele  
(A, B) Lateral view of whole brains. (C, D) Midsagittal views of histological sections. (E, F) Close-up views of the midbrain and metencephalon (boxed in [C] and [D]). (A, C, E) Normal fetus. (B, D, F) Fetus homozygous for mutated I2-derived *Wnt-1* allele. Forebrain components, including the cerebral hemisphere (cr) and thalamus (th), which is derived from the diencephalon, are normal in the mutant. The difference in appearance of the cerebral hemisphere in (A) and (B) is due to shrinkage of the fixed mutant brain (B) relative to the unfixed normal brain (A). Examination of serial sections did not reveal any anatomical or histological difference in the forebrain. The myelencephalon (my) is also normal. However, a large area including most of the midbrain (mb) and the cerebellum (cb) is absent. The pons (po) is present in both the normal and mutant fetuses. The approximate boundary of the area deleted in the mutant is indicated by the arrowheads in (A). Photographs of normal and mutant brains were taken at identical magnifications.

frequencies, which range over three orders of magnitude, will have an important impact on the design of effective targeting vectors for loci, like *Wnt-1*, that fall at the low end of this spectrum.

One of the rate-limiting steps for many targeting experiments has been the reconstruction of mice, owing to clonal variation in the initial population of ES cells used for a gene targeting experiment. This variance is resolved when the cells are cloned. Some clones will efficiently form chimeras, while others will form chimeras very inefficiently, usually with low levels of contribution from the ES

cells. The relative proportion of normal cells in the starting ES cell population will greatly influence the efficiency with which germline transmission can be achieved.

We have used a new ES cell line (AB1) in the experiments described here. The AB1 cell line, and clones derived from it, has proven to be exceptionally stable *in vitro*. We have not observed the clonal variation that has characterized other ES cell lines. To date, we have not identified any clones that fail to contribute to chimeras with high efficiency (90%–100%; Bradley, unpublished data). The differences between AB1 and other ES cell lines are un-

clear, but may reflect the culture conditions or an inherent instability in the available cell lines, since clonal isolates of CCE capable of germline transmission have been shown to progress rapidly to a noneuploid state after cloning (Kuehn et al., 1987; Schwartzberg et al., 1989). As a consequence of the reliability of the AB1 cell line, multiple clones from independent events can be tested with a high probability of success. The use of multiple clones has the distinct advantage that if the same phenotype is observed associated with independent homologous recombination events, then this increases the likelihood that the phenotype results from a targeted disruption rather than a random mutation in another locus. In the experiments reported here, the same phenotype was obtained from two independent clones. Thus, the phenotype almost certainly results from loss of *Wnt-1* activity.

#### The *Wnt-1* Mutant Phenotype

Our initial studies examining *Wnt-1* expression localized *Wnt-1* RNA exclusively to neural tissue from early somite to mid- to late-gestational stages (Wilkinson et al., 1987a). The accuracy of this initial study is confirmed by analysis of the mutant fetuses in this report. In the absence of *Wnt-1*, no phenotype was detected outside of the developing CNS. Moreover, the phenotype, readily distinguishable at 9.5 days (22–24 somites), indicates that *Wnt-1* acts early, in line with the observed expression of *Wnt-1* at 8.5 days.

At 9.5 days it is difficult to accurately define the limits of *Wnt-1* requirement, as there are few useful morphological markers rostral to the hindbrain. However, by examination and extrapolation from mutants observed at 14.5 and 16.5 days, the region that fails to develop includes most of the midbrain and the contiguous rostral metencephalon. The caudal boundary in the metencephalon appears to be dorsoventrally distinct. Dorsally derived cerebellar tissue was not observed, whereas the ventrally derived pons was present. As the cerebellum shares a dual origin from the midbrain and metencephalon (Hallonet et al., 1990), it is presumably possible, if unlikely, that a complete failure of cerebellar development results from loss of the midbrain component. However, the simplest explanation, that the dorsal rostral metencephalon was absent, appears most reasonable.

The anterior boundary is harder to place. At 9.5 days, approximately one-third of the midbrain, presumably the most rostral area, was present. Both dorsal and ventral caudal midbrain were missing. By 14.5 days, the region deleted appeared more substantial. Little, if any, midbrain was observed. These results may reflect an additional loss of rostral midbrain in mutant embryos between 9.5 and 14.5 days. Alternatively, they may reflect different regional growth properties in the midbrain. If, for example, the bulk of the midbrain present in normal fetuses at 14.5 days is derived from the caudal two-thirds of the midbrain of the 9.5-day fetus, the mutants at 14.5 days would appear to have lost significantly more midbrain tissue than at 9.5 days.

The area deleted in mutant mice at 9.5 days was not restricted to the region in which *Wnt-1* is expressed at this

time. *Wnt-1* RNA is normally dorsally restricted at the midline of the midbrain and rostral metencephalon, and in a circle about the midbrain–hindbrain junction (Wilkinson et al., 1987a). These observations can be explained in several ways. *Wnt-1* is a secreted protein (Bradley and Brown, 1990; Papkoff and Schryver, 1990); thus the protein is not restricted to a cell-autonomous action and may be required for normal development over a wide area. Indeed, the *Drosophila* *Wnt-1* gene, *wg*, is required by neighboring cells (DiNardo et al., 1988; Martinez-Arias et al., 1988). Loss of *wg* results in disruption of pattern over an area of the *Drosophila* segment exceeding the narrow band of cells expressing *Wnt-1* RNA. However, in the mouse these distances are much larger than the few cell diameters that make up the *Drosophila* segmental primordia. Moreover, the tenacious association of *Wnt-1* with matrix in vitro (Bradley and Brown, 1990; Papkoff and Schryver, 1990) suggests that in vivo these associations may trap *Wnt-1* locally. Alternatively, *Wnt-1* may be one of a number of signals in a dorsal–ventral signaling cascade required for dorsoventral development in the midbrain. If *Wnt-1* acts as an initial trigger in this pathway, the loss of *Wnt-1* would be postulated to result in the failure of the entire pathway.

Interestingly, the area deleted in *Wnt-1* homozygous mutants at 9.5 days encompasses much, if not all, of the domain in which the mouse *En-1* and *En-2* genes are expressed (Davis et al., 1988; Davis and Joyner, 1988). Earlier studies demonstrated an overlap in expression of *En* and *Wnt-1* RNA at this time (Wilkinson et al., 1987a; Davis et al., 1988; Davis and Joyner, 1988). Thus, both *En* genes, like *Wnt-1*, are expressed in the midbrain, in a circle at the midbrain–hindbrain junction and in the metencephalon. However, the dorsal–ventral domain of *En* expression is more extensive. The correlation between the deleted region in *Wnt-1* mutants and *En* expression is intriguing in view of the regulation of *engrailed* by the *wg* gene in *Drosophila* (DiNardo et al., 1988; Martinez-Arias et al., 1988). Although a thorough examination of *En* expression in fetuses lacking *Wnt-1* activity is necessary, these initial results suggest the exciting possibility that *Wnt-1* regulatory pathways may be evolutionarily conserved.

Examination of the caudal hindbrain and spinal cord in normal fetuses and littermates homozygous for either mutated allele failed to detect any abnormalities in these tissues. However, *in situ* analysis clearly indicates that *Wnt-1* is normally expressed in both these regions of the CNS. The apparent lack of a phenotype in the absence of *Wnt-1* points to functional redundancy among family members. Recent work has revealed that in the mouse the *Wnt-1* family consists of at least eleven members (McMahon and McMahon, 1989; Roelink et al., 1990; Gavin et al., submitted). The expression profiles of only a few of these new genes have been examined in detail. These studies indicate that many other family members are also expressed in the early neural tube (McMahon and McMahon, unpublished data). Thus, the absence of a *Wnt-1* phenotype in the myelencephalon and spinal cord might reflect functional redundancy where expression of a related gene or genes overlaps that of *Wnt-1*. Clearly, a thorough examina-

tion of the expression of other *Wnt* genes is essential to resolve this issue. Interestingly, functional redundancy within the overlapping expression domains of *En-1* and *En-2* has been postulated to explain the absence of an extreme phenotype in mice lacking *En-2* (A. Joyner, personal communication).

#### ***Wnt-1* Function in Neural Development**

The expression of *Wnt-1* in the early somite embryo and the obvious phenotype of mutants at 9.5 days indicate that *Wnt-1* acts early in neural development of the mouse. One explanation for the *Wnt-1* phenotype is that *Wnt-1* may be a determinant required for specifying the region that is deleted in mutants. Alternatively, the *Wnt-1* requirement may be later, associated with the normal growth and development of an already determined region. Finally, *Wnt-1* may be required for both establishment and subsequent development of midbrain and metencephalic tissue. Although we cannot at present distinguish between these alternatives, a consideration of the neural crest may provide some clues to the onset of *Wnt-1* requirement.

The midbrain region is the source of a substantial neural crest component that migrates from the lateral aspect prior to neural tube closure. In the chick, this neural crest population forms the skeleton of both the upper and lower jaw and contributes to the trigeminal ganglion (Noden, 1978a, 1978b; Le Douarin, 1983). In the mammal, observation of migratory pathways (Tan and Morriss-Kay, 1985; Morriss-Kay and Tan, 1987) as well as limited grafting studies (Chan and Tam, 1988) agree with this scheme. The midbrain-derived neural crest in the mouse arises early and is formed over a short period, from about the four to seven somite stages (Chan and Tam, 1988). Thus, if *Wnt-1* acts early in the establishment of regions of the midbrain and metencephalon, then the loss of this tissue might be expected to result in the loss of neural crest with concomitant abnormalities. However, all neural crest components derived from the midbrain were indistinguishable at all stages examined between normal and mutant littermates, supporting the view that *Wnt-1* acts after neural crest migration. It is unlikely that neural crest from other regions substitutes for missing crest, as studies by Noden (1983, 1988) suggest that the fate of the neural crest is predetermined prior to migration and is not reversible. Alternatively, *Wnt-1* may act prior to migration of neural crest cells, but crest precursors may not require *Wnt-1* for normal development. Clearly, to address the important issue of the initial action of *Wnt-1* will require a more detailed examination of both normal *Wnt-1* expression and the onset of the mutant phenotype.

#### **Neurological Consequences of *Wnt-1* Mutation**

The loss of the midbrain and cerebellum in *Wnt-1* mutants has no detrimental effect on *in utero* development. However, no neonate survived beyond 24 hr, despite efforts to swiftly remove competing normal siblings. In view of the substantial area of the CNS deleted, perhaps this is not surprising. Loss of the cerebellum in itself is probably not lethal, as at this time the cerebellum is functionally immature. Moreover, even in adult mice, gross abnormalities in

the cerebellum are not lethal. In the midbrain the deleted region encompasses the area from which the superior and inferior colliculi form. These areas are concerned with visual reflex and the relaying of information in the auditory pathway from the cochlea to the thalamus. Again, loss of these functions is unlikely to result in early neonatal death. Lethality presumably results from massive disruption of the extensive reticular formation as well as the axonal pathways that normally traverse the midbrain in their passage between forebrain, hindbrain, and spinal cord. It will be interesting to explore in these mutants the effect of midbrain deletion on axonal projections, particularly where loss of the target has occurred.

#### **Conclusions**

We have demonstrated that *Wnt-1* is necessary directly or indirectly for the development of a substantial region of the early CNS. Whether *Wnt-1* acts as a determinant for this region or is subsequently required for its normal development remains to be elucidated, as does the pathway(s) of *Wnt-1* action. This report clearly indicates that the role of *Wnt-1* is important, indeed essential, to the survival of offspring. Recent studies by us (McMahon and McMahon, 1989; Gavin et al., submitted) and others (Roe-link et al., 1990) have identified many more *Wnt* family members, all of which are expressed during fetal development. It seems highly likely that the role(s) of these new presumptive cell-signaling proteins will prove equally important.

#### **Experimental Procedures**

##### ***Wnt-1* Homologous Recombination Constructs**

The neomycin resistance cassette used in these experiments was a modification of pMC1neoA (Thomas and Capecchi, 1987). Initially, a neo-tk cassette was constructed by cloning a BgIII-Sall fragment containing 350 bp of rat  $\beta$ -actin promoter (Nudel et al., 1983) driving the expression of HSV-tk into the BamHI-Sall sites just downstream of the polyadenylation signal in pMC1neopolyA. As explained in Results, the actin-tk sequences greatly increased transformation frequencies, presumably owing to enhancement of transcription. A lesser, but significant, enhancement was also obtained using a smaller, 1.45 kb Xhol fragment containing 1.1 kb of pMC1neopolyA (from the Xhol site at 450 to the BamHI site at 1590) with 350 bp of rat  $\beta$ -actin promoter 3' of the BamHI site. The 3' Xhol site was generated by an internal Xhol site in the  $\beta$ -actin promoter just upstream of the cap site (position 274 in Nudel et al., 1983).

The Xhol neo cassette, MC1neoA- $\beta$ -actin, was subcloned into the Xhol site in the second exon of the 10.5 kb BgIII *Wnt-1* genomic clone pMT34 (position 922 in van Ooyen and Nusse, 1984) previously subcloned into the BamHI-BgIII sites of pSP72 (Promega). pSP72 MT34 contains the entire *Wnt-1* gene, approximately 6.5 kb of 5' sequence upstream of the cap site, and all four *Wnt-1* introns in the 4.0 kb transcription unit. Insertion of the neo cassette occurs within the coding sequence, disrupting the *Wnt-1* gene. The transcriptional orientation of the cassette was the same as that of *Wnt-1*. HSV-tk sequences were then attached at either end for negative selection against nonhomologous recombinants (Mansour et al., 1988).

A construct containing the MC1 polyoma enhancer driving tk expression was made by cloning a Xhol-EcoRI fragment (450-828) of pMC1neoA into a Sall- and EcoRI-cut subclone of HSV-tk (EcoRI-PvuII; McKnight, 1980) in pKS (Stratagene). Digesting this subclone with Sall and XbaI excised the MC1TK cassette and allowed insertion of this fragment in the unique Sall-XbaI sites in the polylinker of pSP72MT34 5' of the *Wnt-1* genomic sequences. This construct was then cut with ClaI, which cleaves 5' of the HSV-tk sequences, in pKS-donated polylinker sequence, and in a unique ClaI site in the third exon

of *Wnt-1* (1846 in van Ooyen and Nusse, 1984) 921 nucleotides downstream of the MC1/neopA- $\beta$ -actin insertion site. This *Clai* fragment was then subcloned into the unique *Clai* site in pKSMC1TK and the orientation of insertion determined. The final construct, designated p401 (Figure 1), contains MC1TK sequences at either end of the *Wnt-1* genomic sequence, both of which are in the opposite transcriptional orientation to *Wnt-1* (see Figure 1). Two unique sites, *NotI* and *Sall*, allow the construct to be linearized. *Sall*-linearized DNA was used for transfection.

#### Cell Lines

The AB1 cell line was derived from a Black Agouti 129 mouse embryo using standard procedures and was checked for the presence of the Y chromosome and the ability to generate germline chimeras by blastocyst injection (data not shown).

AB1 cells were cultured as previously described (Robertson, 1987) on mitotically inactive SNL76/7 feeder cells. SNL76/7 cells were clonally derived from a STO cell line transfected with a G418<sup>R</sup> cassette (RV4.0; Thomas and Capecchi, 1987) and a LIF expression construct (Williams et al., 1988). SNL76/7 are both G418<sup>R</sup> and express LIF at an abundant level.

#### Transfection and Selection

Cells were collected from trypsinized confluent 9 cm plates approximately 3 hr after refeeding. Following centrifugation, they were resuspended directly in PBS ( $\text{Ca}^{2+}$  and  $\text{Mg}^{2+}$  free) at a cell density of  $1.2 \times 10^7/\text{ml}$  and a DNA concentration of 25  $\mu\text{g}/\text{ml}$ . Electroporation (Bio-Rad electroporator) of a 0.9 ml aliquot of cells and DNA was carried out at 230 V, 500  $\mu\text{F}$  once, and 240 V, 500  $\mu\text{F}$  once at room temperature. Immediately after transfection, each 0.9 ml aliquot was plated onto a 90 mm feeder plate. G418 (350  $\mu\text{g}/\text{ml}$  dry powder; Gibco) and FIAU (0.2  $\mu\text{M}$  1-[2-deoxy, 2-fluoro- $\beta$ -D-arabinofuranosyl]-5 iodouracil; Bristol Myers) selection was applied 24 hr after plating without subculture and allowed to proceed for 9–12 days.

#### PCR—Identification of Homologous Recombinant Clones

PCR conditions (Saiki et al., 1985) were established on cells that had previously been transfected with a control construct. Cells were lysed at 55°C in 50–100  $\mu\text{l}$  of lysis buffer: 50 mM KCl, 1.5 mM  $\text{MgCl}_2$ , 10 mM Tris (pH 8.5) (25°C), 0.01% gelatin, 0.45% NP40, 0.45% Tween 20, and 100  $\mu\text{g}/\text{ml}$  proteinase K for 12–16 hr. The proteinase K was inactivated at 94°C for 15 min. PCR was carried out in the following mixture in a 50  $\mu\text{l}$  final volume: 50 mM KCl, 1.5 mM  $\text{MgCl}_2$ , 1 mM Tris (pH 8.3), 0.01% gelatin, 5% DMSO, 250  $\mu\text{M}$  of each dNTP, 100 ng of each primer, and 2 U of Taq polymerase (Cetus). Temperature cycling was as follows: 93°C, 30 sec; 70°C, 1 min; 72°C, 1 min; repeated 35 times.

The following oligonucleotides were used to identify *Wnt-1* homologous recombinants: rat  $\beta$ -actin sense oligonucleotide 1480 (5'-CGGG-CGAGGCCGGTGAGTGAGCG-3'; positions 205–227 in Nudel et al., 1983); *Wnt-1* sense oligonucleotide 1113 (5'-AAGCAGCGCGACTGA-TCCGACAG-3'; positions 952–975 in van Ooyen and Nusse, 1984); *Wnt-1* antisense oligonucleotide 1114 (5'-GAACCTCTCGGCCAAAGAG-GCGACCA-3'; positions 1878–1854 in van Ooyen and Nusse, 1984). Oligonucleotides 1480 and 1114 amplify a 1025 bp PCR product only on integration of p401 into the *Wnt-1* locus. PCR products were resolved on 1% agarose gels, vacuum-blotted to GeneScreen Plus membrane (Du Pont) in 0.4 N NaOH, and probed with the internal oligonucleotide 1113 to confirm the identification of amplified bands. Oligonucleotide hybridization was for 1 hr at 65°C in 1.5× SSPE, 1% SDS, 600  $\mu\text{g}/\text{ml}$  sheared single-stranded DNA, 0.5% nonfat milk powder, and 30 ng/ml kinased oligonucleotide. Washes were performed at 37°C in 6× SSC, 1% SDS, three times for 5 min each. In all cases the prominent 1025 bp band visible after ethidium bromide staining of gels hybridized specifically to oligonucleotide 1113. Additional bands were not detected by the oligonucleotide probe. Heterozygous animals were detected by allele-specific PCR of blood collected from the tail. Approximately 2  $\mu\text{l}$  of blood was collected directly into 500  $\mu\text{l}$  of isotonic buffer (250 mM sucrose, 30 mM NaCl, 2 mM  $\text{CaCl}_2$ , 50 mM Tris [pH 7.5]). Red cells were lysed by the addition of Triton X-100 to 1%, and white cell nuclei were sedimented by centrifugation. Nuclei were lysed for PCR by addition of PCR lysis buffer and processed as described for ES cells.

#### PCR Controls

ES cells were transfected with a positive control construct that contained additional 3' flanking sequence not present on the plasmid used for targeting. G418<sup>R</sup> clones were obtained and expanded as a population. Once confluent, the cells were lysed at a cell density of  $6 \times 10^6/\text{ml}$  in PCR lysis buffer and proteinase K treated for 12–16 hr at 55°C; the proteinase K was inactivated at 94°C for 15 min. DNA prepared from the positive control cells was subjected to PCR under standard conditions at a variety of different dilutions both with and without an excess of wild-type genomic DNA. Under the conditions described, we were able to detect on an ethidium bromide-stained agarose gel a specific PCR product from as few as 10 positive cells in the presence of genomic DNA from  $10^4$  wild-type cells.

#### Generation of Chimeric Mice

Manipulations were carried out exactly as described by Bradley (1987). Briefly, 10–15 ES cells were injected into the blastocoelic cavity of C57BL/6J embryos at 3.5 days postcoitum. After injection, the embryos were allowed to recover for 30–60 min before surgical transfer to the uteri of pseudopregnant recipients at 2.5 days postcoitum. Pups were born 17 days after injection and identified visually as chimeric on the basis of agouti pigmentation in the coat 10 days later. Chimeric males were set up to breed at 6 weeks of age with C57BL/6J females. Germinal transmission was scored on the basis of allele-specific PCR of blastocyst outgrowths after 3 days of in vitro culture and/or on the presence of agouti pigmentation in the coat of F1 animals 10 days after birth.

#### Southern Blot Analysis of Integration Sites and Genotyping of Progeny

DNA was isolated from the AB1 cell line and from each of the recombinant ES cell lines positive for homologous recombination by PCR. DNA was subjected to restriction enzyme digestion with *SacI*, *BglII*, *SphI*, and *StuI*. Approximately 2.5  $\mu\text{g}$  of each digest was fractionated on a 0.8% agarose gel, transferred to GeneScreen (DuPont), and hybridized with a 1263 bp *Clai*-Mu1 (Figure 2, positions 704–1966 in Fung et al., 1985) *Wnt-1* cDNA probe. As genomic sequences present in p401 end at this *Clai* site, there is no overlap between this probe and sequences present in p401. In addition, blots were also screened with a *neo* and HSV-tk probe. DNA was prepared from yolk sacs of day 9.5 and day 16.5 fetuses and tails of newborn offspring from matings between heterozygous individuals. All the yolk sac DNA from day 9.5 fetuses and approximately 5  $\mu\text{g}$  from each of the other samples was digested with *SacI*, fractionated on a 0.7% agarose gel, transferred to GeneScreen, and hybridized with the flanking *Wnt-1* cDNA probe. Hybridization and wash conditions were according to the manufacturer's recommendations with final washes in 0.2× SSC at 68°C.

#### Histological Analysis

Fetal samples were fixed in 4% paraformaldehyde in PBS overnight and processed as described by Wilkinson et al. (1987b). Sections were stained using Masson's trichrome with (day 9.5 and day 14.5 samples) or without (day 16.5 sample) prior treatment with Alcian blue. All photomicrography was performed on a Leitz Aristoplan photomicroscope using Kodak Technical Pan 2145.

#### Acknowledgments

We would like to thank Paul Hasty for constructing the MC1 tk cassette, Glenn Friedrich for mapping enhancer elements in MC1neo- $\beta$ -actin-tk, and Drew Noden for valuable discussion of the results. We are indebted to Jill McMahon for speedy histology under trying conditions and to all those in the animal facilities of Hoffmann-La Roche Inc. and Baylor College who facilitated this analysis. We thank Marie Wims and J. D. Wallace for expert technical assistance and Robert Preston for technical assistance with the mice. We are indebted to one of the reviewers for the careful reading and helpful suggestions. We also thank Alice O'Connor for her rapid preparation of the manuscript.

A. P. McM. was supported by the Roche Institute of Molecular Biology, Roche Research Center, Hoffmann-La Roche Inc., Nutley, NJ. A. B. was supported by grants from the National Institutes of Health (HD24613 and HD25326), the Cystic Fibrosis Foundation, and the

Searle Scholars Trust. Core support was provided by the Baylor MRRC 5 P30 HD24064 from the Institute of Child Health and Development.

The costs of publication of this article were defrayed in part by the payment of page charges. This article must therefore be hereby marked "advertisement" in accordance with 18 USC Section 1734 solely to indicate this fact.

Received August 8, 1990; revised August 20, 1990.

## References

- Baker, N. E. (1987). Molecular cloning of sequences from *wingless*, a segment polarity gene in *Drosophila*; the spatial distribution of a transcript in embryos. *EMBO J.* 6, 1765–1770.
- Baker, N. E. (1988). Embryonic and imaginal requirements for *wingless*, a segment polarity gene in *Drosophila*. *Dev. Biol.* 125, 96–108.
- Bradley, A. (1987). Production and analysis of chimaeric mice. In *Teratocarcinomas and Embryonic Stem Cells: A Practical Approach*, E. J. Robertson, ed. (Oxford: IRL Press), pp. 113–151.
- Bradley, A., Evans, M. J., Kaufman, M. H., and Robertson, E. J. (1984). Formation of germ-line chimaeras from embryo-derived teratocarcinoma cell lines. *Nature* 309, 255–256.
- Bradley, R. S., and Brown, A. M. C. (1990). The proto-oncogene *int-1* encodes a secreted protein associated with the extracellular matrix. *EMBO J.* 9, 1569–1575.
- Cabrera, C. V., Alonso, M. C., Johnston, P., Phillips, R. G., and Lawrence, P. A. (1987). Phenocopies induced with antisense RNA identify the *wingless* gene. *Cell* 50, 658–663.
- Chan, W. Y., and Tam, P. P. L. (1988). A morphological and experimental study of the mesencephalic neural crest cells in the mouse embryo using wheat germ agglutinin–gold conjugate as the cell marker. *Development* 102, 427–442.
- Charron, J., Malynn, B. A., Robertson, E. J., Goff, S. P., and Alt, F. W. (1990). High-frequency disruption of the *N-myc* gene in embryonic stem and pre-B cell lines by homologous recombination. *Mol. Cell. Biol.* 10, 1799–1804.
- Davis, C. A., and Joyner, A. L. (1988). Expression patterns of the homeo box-containing genes *En-1* and *En-2* and the proto-oncogene *int-1* diverge during mouse development. *Genes Dev.* 2, 1736–1744.
- Davis, C. A., Noble-Topham, S. E., Rossant, J., and Joyner, A. L. (1988). Expression of the homeo box-containing gene *En-2* delineates a specific region of the developing mouse brain. *Genes Dev.* 2, 361–371.
- DeChiara, T. M., Efstratiadis, A., and Robertson, E. J. (1990). A growth-deficiency phenotype in heterozygous mice carrying an insulin-like growth factor II gene disrupted by targeting. *Nature* 345, 78–80.
- DiNardo, S., Sher, E., Heemskerk-Jongens, J., Kassis, J. A., and O'Farrell, P. H. (1988). Two-tiered regulation of spatially patterned *engrailed* gene expression during *Drosophila* embryogenesis. *Nature* 332, 604–609.
- Evans, M. J., and Kaufman, M. H. (1981). Establishment in culture of pluripotential cells from mouse embryos. *Nature* 292, 154–156.
- Fung, Y.-K. T., Shackleford, G. M., Brown, A. M. C., Sanders, G. S., and Varmus, H. E. (1985). Nucleotide sequence and expression *in vitro* of cDNA derived from mRNA of *int-1*, a provirally activated mouse mammary oncogene. *Mol. Cell. Biol.* 5, 3337–3344.
- Hallonet, M. E. R., Teillet, M.-A., and Le Douarin, N. M. (1990). A new approach to the development of the cerebellum provided by the quail–chick marker system. *Development* 108, 19–31.
- Jakobovits, A., Shackleford, G. M., Varmus, H. E., and Martin, G. R. (1986). Two proto-oncogenes implicated in mammary carcinogenesis, *int-1* and *int-2*, are independently regulated during mouse development. *Proc. Natl. Acad. Sci. USA* 83, 7806–7810.
- Johnson, R. S., Sheng, M., Greenberg, M. E., Kolodner, R. D., Papaioannou, V. E., and Spiegelman, B. M. (1989). Targeting of nonexpressed genes in embryonic stem cells via homologous recombination. *Science* 245, 1234–1236.
- Joyner, A. L., Skarnes, W. C., and Rossant, J. (1989). Production of a mutation in the mouse *En-2* gene by homologous recombination in embryonic stem cells. *Nature* 338, 153–156.
- Koller, B. H., and Smithies, O. (1989). Inactivating the  $\beta_2$ -microglobulin locus in mouse embryonic stem cells by homologous recombination. *Proc. Natl. Acad. Sci. USA* 86, 8932–8935.
- Kuehn, M. R., Bradley, A., Robertson, E. J., and Evans, M. J. (1987). A potential animal model for Lesch–Nyhan syndrome through introduction of HPRT mutations into mice. *Nature* 326, 295–298.
- Le Douarin, N. M. (1983). *The Neural Crest* (Cambridge: Cambridge University Press).
- Mansour, S. L., Thomas, K. R., and Capecchi, M. R. (1988). Disruption of the proto-oncogene *int-2* in mouse embryo-derived stem cells: a general strategy for targeting mutations to non-selectable genes. *Nature* 336, 348–352.
- Martinez-Arias, A., Baker, N. E., and Ingham, P. W. (1988). Role of segment polarity genes in the definition and maintenance of cell states in the *Drosophila* embryo. *Development* 103, 157–170.
- McKnight, S. L. (1980). The nucleotide sequence and transcript map of the herpes simplex virus thymidine kinase gene. *Nucl. Acids Res.* 8, 5949–5964.
- McMahon, A. P., and Moon, R. T. (1989). *int-1*—a proto-oncogene involved in cell signalling. *Development* 107 (Suppl.), 161–167.
- McMahon, J. A., and McMahon, A. P. (1989). Nucleotide sequence, chromosomal localization and developmental expression of the mouse *int-1*-related gene. *Development* 107, 643–651.
- Morata, G., and Lawrence, P. A. (1977). The development of *wingless*, a homeotic mutation of *Drosophila*. *Dev. Biol.* 56, 227–240.
- Morriss-Kay, G., and Tan, S.-S. (1987). Mapping cranial neural crest cell migration pathways in mammalian embryos. *Trends Genet.* 3, 257–261.
- Noden, D. M. (1978a). The control of avian cephalic neural crest cytotdifferentiation. I. Skeletal and connective tissues. *Dev. Biol.* 67, 296–312.
- Noden, D. M. (1978b). The control of avian cephalic neural crest cytotdifferentiation. II. Neural tissues. *Dev. Biol.* 67, 313–329.
- Noden, D. M. (1983). The role of the neural crest in patterning of avian cranial skeletal, connective, and muscle tissues. *Dev. Biol.* 96, 144–165.
- Noden, D. M. (1988). Interactions and fates of avian craniofacial mesenchyme. *Development* 103 (Suppl.), 121–140.
- Nudel, U., Zakut, R., Shani, M., Neuman, S., Levy, Z., and Yaffe, D. (1983). The nucleotide sequence of the rat cytoplasmic  $\beta$ -actin gene. *Nucl. Acids Res.* 11, 1759–1771.
- Nusse, R. (1988). The activation of cellular oncogenes by proviral insertion in murine mammary tumors. In *Breast Cancer: Cellular and Molecular Biology*, M. E. Lippman and R. Dickson, eds. (Boston: Kluwer Academic Publishers), pp. 283–306.
- Nusse, R., and Varmus, H. E. (1982). Many tumors induced by mouse mammary tumor virus contain a provirus integrated in the same region of the host chromosome. *Cell* 31, 99–109.
- Nüsslein-Volhard, C., and Wieschaus, E. (1980). Mutations affecting segment number and polarity in *Drosophila*. *Nature* 287, 795–801.
- Papkoff, J. (1989). Inducible overexpression and secretion of *int-1* protein. *Mol. Cell. Biol.* 9, 3377–3384.
- Papkoff, J., and Schryver, B. (1990). Secreted *int-1* protein is associated with the cell surface. *Mol. Cell. Biol.* 10, 2723–2730.
- Rijsewijk, F., Schuermann, M., Wagenaar, E., Parren, P., Weigel, D., and Nusse, R. (1987). The *Drosophila* homolog of the mouse mammary oncogene *int-1* is identical to the segment polarity gene *wingless*. *Cell* 50, 649–657.
- Robertson, E. J. (1987). Embryo-derived stem cell lines. In *Teratocarcinomas and Embryonic Stem Cells: A Practical Approach*, E. J. Robertson, ed. (Oxford: IRL Press), pp. 71–112.
- Roelink, H., Wagenaar, E., Lopes da Silva, S., and Nusse, R. (1990). *wnt-3*, a gene activated by proviral insertion in mouse mammary tumors, is homologous to *int-1/wnt-1* and is normally expressed in mouse embryos and adult brain. *Proc. Natl. Acad. Sci. USA* 87, 4519–4523.
- Saiki, R. K., Scharf, S., Faloona, F., Mullis, K. B., Horn, G. T., Erlich, H. A., and Arnheim, N. (1985). Enzymatic amplification of  $\beta$ -globin

- genomic sequences and restriction site analysis for diagnosis of sickle cell anemia. *Science* 230, 1350–1354.
- Schwartzberg, P. L., Goff, S. P., and Robertson, E. J. (1989). Germ-line transmission of a *c-abl* mutation produced by targeted gene disruption in ES cells. *Science* 246, 799–804.
- Shackleford, G. M., and Varmus, H. E. (1987). Expression of the proto-oncogene *int-1* is restricted to postmeiotic male germ cells and the neural tube of mid-gestation embryos. *Cell* 50, 89–95.
- Sharma, R. P. (1973). *Wingless*, a new mutant in *D. melanogaster*. *Dros. Inf. Serv.* 50, 134.
- Sharma, R. P., and Chopra, V. L. (1976). Effect of *wingless* (*wg*) mutation on wing and haltere development in *Drosophila melanogaster*. *Dev. Biol.* 48, 461–465.
- Tan, S.-S., and Morris-Kay, G. (1985). The development and distribution of the cranial neural crest in the rat embryo. *Cell Tissue Res.* 240, 403–416.
- Thomas, K. R., and Capecchi, M. R. (1987). Site-directed mutagenesis by gene targeting in mouse embryo-derived stem cells. *Cell* 51, 503–512.
- Thompson, S., Clarke, A. R., Pow, A. M., Hooper, M. L., and Melton, D. W. (1989). Germ line transmission and expression of a corrected HPRT gene produced by gene targeting in embryonic stem cells. *Cell* 56, 313–321.
- Tsukamoto, A. S., Grosschedl, R., Guzman, R. C., Parslow, T., and Varmus, H. E. (1988). Expression of the *int-1* gene in transgenic mice is associated with mammary gland hyperplasia and adenocarcinomas in male and female mice. *Cell* 55, 619–625.
- van den Heuvel, M., Nusse, R., Johnston, P., and Lawrence, P. A. (1989). Distribution of the *wingless* gene product in *Drosophila* embryos: a protein involved in cell-cell communication. *Cell* 59, 739–749.
- van Ooyen, A., and Nusse, R. (1984). Structure and nucleotide sequence of the putative mammary oncogene *int-1*; proviral insertions leave the protein-encoding domain intact. *Cell* 39, 233–240.
- Wilkinson, D. G., Bailes, J. A., and McMahon, A. P. (1987a). Expression of the proto-oncogene *int-1* is restricted to specific neural cells in the developing mouse embryo. *Cell* 50, 79–88.
- Wilkinson, D. G., Bailes, J. A., Champion, J. E., and McMahon, A. P. (1987b). A molecular analysis of mouse development from 8 to 10 days post coitum detects changes only in embryonic globin expression. *Development* 99, 493–500.
- Wilkinson, D. G., Bailes, J. A., and McMahon, A. P. (1989). Expression of proto-oncogene *int-1* is restricted to specific regions of the developing mouse neural tube. In *Cell to Cell Signals in Mammalian Development*, NATO ASI Series, Vol. H26 (Berlin: Springer-Verlag), pp. 311–317.
- Williams, R. L., Hilton, D. J., Pease, S., Willson, T. A., Stewart, C. L., Gearing, D. P., Wagner, E. F., Metcalf, D., Nicola, N. A., and Gough, N. M. (1988). Myeloid leukaemia inhibitory factor maintains the developmental potential of embryonic stem cells. *Nature* 336, 685–687.
- Zijlstra, M., Li, E., Sajiadi, F., Subramani, S., and Jaenisch, R. (1989). Germ-line transmission of a disrupted  $\beta_2$ -microglobulin gene produced by homologous recombination in embryonic stem cells. *Nature* 342, 435–438.

